104 (2025) 105772

Contents lists available at ScienceDirect

Poultry Science

journal homepage: www.elsevier.com/locate/psj

Full-Length Article

Zn glycine mitigates the LPS-induced hepatic injury and inflammation through NrF2/NFκB signaling in geese

Zeshan Zulfiqar [a,1], Muhammad Arslan Asif [a,1], Layla Al-Mitib [d], Khawla Alharbi [d], Tanzina Hossain [e], Han Yao [a], Xiaoyan Zhu [a,b,c], Zhichang Wang [a,b,c], Hao Sun [a,b,c], Yalei Cui [a,b,c], Boshuai Liu [a,b,c,*], Yinghua Shi [a,b,c,*]

[a] Department of Animal Nutrition and Feed Science, College of Animal Science, Henan Agricultural University, Zhengzhou, China
[b] Henan Key Laboratory of Innovation and Utilization of Grassland Resources, Zhengzhou, China
[c] Henan Forage Engineering Technology Research Center, Zhengzhou, Henan 450002, China
[d] Department of Biological Sciences, University of Arkansas, Fayetteville, AR 72701, USA
[e] Department of Applied Food Science and Nutrition, Chattogram Veterinary and Animal Sciences University (CVASU), Chattogram, Bangladesh

ARTICLE INFO

Keywords:
LPS
Inflammation
Liver
Zn_Gly
Geese

ABSTRACT

Gram-negative bacteria like *Escherichia coli* have an outer membrane that contains lipopolysaccharide (LPS), which is a powerful inducer of systemic inflammation. It is often associated with gut dysbiosis, intestinal barrier dysfunction, and liver damage. Despite increasing recognition of the gut–liver axis as a critical mediator in systemic inflammation and hepatic pathology, the efficacy of nutritional strategies targeting this pathway remains inadequately defined. This study evaluated the protective effects of zinc glycine (Zn_Gly), a highly bioavailable organic zinc chelate, against LPS-induced gut barrier disruption and liver damage in meat geese. Zn_Gly supplementation @ 80mg/kg of diet significantly attenuated LPS-induced impairments in growth performance, gut morphology, intestinal permeability and liver damage. Zn_Gly reduced considerably ($p < 0.01$) the levels of LPS in the both liver and ceca, and significantly increased ($p < 0.01$) the expression of tight junction proteins (ZO-1, CLDN-1), thereby mitigating LPS translocation and systemic inflammation (IL-1β, IL-18 and TNF-α) by increasing IL-10 production. Notably, Zn_Gly reversed LPS-mediated oxidative stress by enhancing hepatic antioxidant enzyme activities (**SOD, CAT, GSH-Px, T-AOC**; $p < 0.01$) and reducing oxidative markers (**ROS, MDA, TBARS**). Crucially, Zn_Gly mitigated the adverse effects of LPS on liver health by improving ALT, AST, IgG and IgA significantly ($p < 0.01$) leading to reduced Ishaq pathology score and disease related histological parameters. Zn_Gly also improved the hepatic liver metabolism through increasing β-oxidation. Concurrently, Zn_Gly promoted antioxidant defense mechanism NrF2 through upregulation of markers (**H0-1, NQO-1 & GCLM**). In terms of mechanism, these effects were brought about by blocking the NF-κB signaling pathway, which is essential for the inflammatory liver damage caused by LPS. These findings elucidate Zn_Gly as a promising nutritional modulator of the gut–liver axis, attenuating systemic inflammation and conferring protection against inflammation-induced liver damage. This underscores its therapeutic potential for improving animal health and guiding translational strategies in metabolic disorders associated with gut and hepatic dysfunction.

Introduction

The gut-liver axis represents a crucial physiological interface that integrates metabolic, immunological, and microbial signals. The portal vein connects the liver to the intestine, and it is continuously exposed to metabolites, microbial products, and antigens from the gut. Under healthy conditions, this communication promotes immune tolerance and metabolic homeostasis. However, disruption of intestinal barrier function or microbial imbalance (dysbiosis) can lead to the endotoxins' translocation such as lipopolysaccharide (LPS), triggering hepatic inflammation and injury (Albillos et al., 2020). Gram-negative bacteria's outer membrane contains LPS, a powerful innate immune system

* Corresponding authors at: Department of Animal Nutrition and Feed Science, College of Animal Science, Henan Agricultural University, Zhengzhou, China.
E-mail addresses: boshuailiu@126.com (B. Liu), annysyh@henau.edu.cn (Y. Shi).
[1] These authors contributed equally to this work.

https://doi.org/10.1016/j.psj.2025.105772
Received 14 July 2025; Accepted 2 September 2025
Available online 3 September 2025

stimulant that mainly acts via Toll-like receptor 4 (TLR4) and its downstream effector, nuclear factor-kappa B (NF-κB). NF-κB activation leads to the transcription of numerous pro-inflammatory cytokines, including TNF-α, IL-1β, and IL-6, contributing to hepatic damage and systemic inflammation (Wang et al., 2023).

Oxidative stress also contributes to liver damage in a synergistic way, as the excessive generation of reactive oxygen species (ROS) exacerbates cellular damage and inflammatory signaling (Allameh et al., 2023). Nuclear factor erythroid 2–related factor 2 (Nrf2) is a transcription factor that mediates cellular antioxidant defenses by upregulating the expression of several antioxidant enzymes including heme oxygenase-1 (HO-1), superoxide dismutase (SOD), and glutathione peroxidase (GSH-Px) described by Tonelli et al. (2018). The crosstalk between the Nrf2 and NF-κB pathways is critical in determining the balance between pro-inflammatory and cytoprotective responses during hepatic stress.

Zinc (Zn) is a trace element essential for maintaining cellular integrity, immune function, and antioxidant defenses (Wessels et al., 2017). In the context of liver health, zinc plays a multifaceted role. It is an essential component for many antioxidant enzymes that shield hepatocytes from oxidative damage, including SOD (Prasad and Bao, 2019; Martins et al., 2022). Zinc also stabilizes cellular membranes and maintains the structural integrity of hepatocytes under stress conditions (Kusanaga et al., 2019). Furthermore, zinc regulates apoptosis and promotes hepatocyte proliferation, thereby contributing to liver regeneration after injury (Aksoy-Ozer et al., 2024). Zinc has been demonstrated to reduce hepatic inflammation by preventing Kupffer cell activation and the synthesis of pro-inflammatory cytokines like TNF-α and IL-1β. (Von Bülow et al., 2007; Zhang et al., 2021). Chronic liver illnesses, such as fibrosis and non-alcoholic fatty liver disease (NAFLD), zinc deficiency is often correlated with disease progression, oxidative stress, and impaired liver function (Mohammad et al., 2012). Zinc's immunomodulatory properties are well documented, but recent advances highlight that the chemical form of zinc significantly influences its bioavailability and efficacy. Organic zinc complexes, such as zinc glycine (Zn_Gly), where zinc is chelated with the amino acid glycine, exhibit superior absorption and stability compared to traditional inorganic forms (Chang et al., 2023). Importantly, glycine itself possesses anti-inflammatory, immunomodulatory, and cytoprotective properties (Zhong et al., 2003), making Zn_Gly a dual-function compound with potential synergistic effects on gut and liver health.

The precise effects of Zn_Gly on the gut-liver axis are not well understood, despite the increased interest in using organic zinc in animal feeding, particularly under inflammatory conditions. Moreover, most studies have been conducted in mammalian models, with limited data available for avian species. Geese represent a unique model due to their distinctive hepatic metabolism (Ren et al., 2024), including a high capacity for lipid deposition and a heightened sensitivity to endotoxin-induced liver injury. Understanding how dietary interventions like Zn_Gly influence the gut-liver axis in geese not only provides insights into avian physiology but also has practical implications for poultry health management and disease prevention.

The purpose of this study was to look into how Zn_Gly protects geese against liver damage caused by LPS, with a particular focus on the Nrf2/NF-κB signaling pathways. By elucidating the molecular mechanisms underlying Zn_Gly's action, we aimed to demonstrate its potential as a cutting-edge dietary approach to reduce oxidative stress and inflammation along the gut-liver axis.

Material and methods

Ethical approval

The Henan Agricultural University Animal Welfare Committee (Approval No. HNND2023082705), located in Zhengzhou, China, authorized the protocols for all animal procedures, nutritional treatments, and sampling.

Animal, diets and experimental design

Male wanpu geese of day-old age were divided into three treatment groups at random (six replicates per group, each replicate comprises 10 geese): the LPS-challenged group (LPS), the non-challenged control group (CON), and the LPS-challenged group supplemented with 80 mg/kg of zinc glycine (LPS + Zn_Gly). Our earlier research served as the basis for the best chosen Zn supplementation level (Zulfiqar et al., 2025). The experiment lasted for 21 days. On day 15th, A 0.5 mL injection of LPS was given to geese in the LPS group (1 mg/kg BW; 1.2880, *E.coli* 055:B5; Sigma-Aldrich, St. Louis, MO, USA) twice 8 h apart, while 0.9 % sterile saline was administered into the CON group. The feed company's guidance was followed when establishing the basal diet and Table 1 provides a detailed overview of its composition and nutritional content. All geese were housed in controlled environment with unlimited access to pelleted feed and water. The room temperature was kept at 33 ± 1°C for the first week and each week, it was lowered by 3°C thereafter, reaching 24 ± 1 °C by the third week. Relative humidity was maintained at 65–75 %, and lighting was continuous throughout the experiment. Chelota Group supplied the Zn_Gly used in this study (Guanhan, China) and contained 21 % Zn with a purity of 98.5 %. All experimental birds were obtained from Henan Daidai goose Agriculture and Animal husbandry development Co. LTD Zhumadian, China.

Sample collection

At the end of the 21-day trial, three geese per replicate pen were selected for sampling. Birds chosen had body weights closest to the pen's mean body weight to ensure representativeness. Selected geese were anesthetized with sodium pentobarbital (30 mg/kg BW, intravenous) prior to euthanasia. For histopathological examination, tissues and cecal were gathered and promptly preserved in 4 % paraformaldehyde. Furthermore, liver and cecal samples were stored in cryogenic tubes, quickly frozen in liquid nitrogen, and kept at −80°C for further examination of biomarkers linked to gut-liver inflammation and barrier function. Upon completion of 21 days, geese having BW nearest to the mean within every group receiving treatment were chosen for intestinal permeability evaluation. The geese were given fluorescein

Table 1
Composition of feed used in the study.

Ingredients %	0-21 d
Maize	57.8
Wheat Bran	5.0
Soybean Meal (43.5 %)	30
Rice Husk	1.3
Sunflower meal	2.00
Limestone	1.1
DCP	1.4
Lysine	0.04
DL-methionine	0.1
Premix	1
Salt	0.3
Calculated Values	
ME (Kcal/Kg)	2726
Crude Protein (CP)	19.03
Crude Fiber	4.50
Calcium	0.83
Total Phosphorus	0.65
Lysine	0.92
Methionine	0.37
Zinc, mg/kg	35.41

Premix provided per kilogram of diet: vitamin A, 2000 IU; vitamin D3, 45000 U; vitamin E, 300IU; vitamin K3, 20 mg; vitamin B1, 10 mg; vitamin B2, 120 mg; vitamin B6, 20 mg; nicotinic acid, 600 mg; pantothenic acid, 180 mg; folic acid, 10 mg; choline, 7 g; Fe, 1.2 g; Cu, 0.2 g; Mn, 1.9 g; I, 10 mg; Se, 6 mg. Zn contents was a measured data, while others nutrient levels were calculated. data.

isothiocyanate-dextran (FITC-D; molecular weight: 3-5 kDa; Sigma-Aldrich, St. Louis, MO, USA) via oral gavage at a dose of 4.16 mg/kg BW and blood samples were collected 2 h later for fluorescence analysis. The replicate pen served as the experimental unit in all statistical analyses.

Growth performance

The geese in each replication were measured for fasting body weight on days 1, 14, and 21 of the experiment. Concurrently, feed intake and residual feed were measured to determine feed consumption. The feed-to-gain ratio (F/G), average daily gain (ADG), and average daily feed intake (ADFI) were computed for every replication based on these data. Liver index was measured by dividing the liver weight with total body weight.

FITC-D and D-LA analysis

Fluorescein isothiocyanate–dextran (FITC-D) and D-lactic acid (D-LA), indicators of intestinal permeability, were determined by centrifuging serum samples at 500 × *g* for 15 minutes and then storing them at −20°C. FITC-D fluorescence in plasma was measured using the methodology outlined by Vicuña et al. (2015). The concentration of D-LA was determined using a commercial enzyme-linked immunosorbent assay (ELISA) kit (MM-91646O1; Jiangsu Meimian Industrial Co., Ltd., Jiangsu, China).

Measurement of tight junction proteins

Cecal tissues from geese were carefully dissected and immediately fixed in 4 % paraformaldehyde at 4°C for 24 h. Following fixation, using phosphate-buffered saline (PBS), tissues were cleaned and either processed for paraffin embedding or cryopreservation. Tissues were cleaned in xylene, dehydrated using graded alcohols, and then embedded in paraffin for paraffin embedding. A microtome was used to cut sections that were 5 μm thick. The sections were then put on positively charged glass slides and allowed to dry. For cryosections, tissues were cryoprotected in 30 % sucrose overnight, embedded in OCT compound, and sectioned at 5–10 μm thickness using a cryostat. Paraffin sections underwent deparaffinization in xylene, rehydration through a graded ethanol series, and antigen retrieval using citrate buffer (pH 6.0) at 95–100°C for 20 min, followed by cooling and PBS washes. Both paraffin and cryosections were permeabilized and blocked using 5 % bovine serum albumin (BSA) or 10 % serum from normal goat containing 0.1 % Triton X-100 in phosphate buffer solution for 1 hour at ambient temperature in a humidified place to reduce nonspecific binding. Primary antibodies against tight junction proteins ZO-1 (rabbit anti-ZO-1, Servicebio China, Cat. No. GB111402, 1:500) and Claudin-1 (rabbit anti-Claudin-1, Servicebio, China, Cat. No. GB12032, 1:500) were diluted in blocking buffer and applied to the tissue sections. The slides were stored in a humidified room at 4°C for the whole night. On the next day, the sections were rinsed three times with PBS, each wash lasting 5 minutes. Fluorophore-conjugated secondary antibodies (Alexa Fluor 488-conjugated anti-rabbit IgG, Servicebio, Cat. No. GB21303, 1:300) were diluted in blocking buffer and applied to sections for 60 minutes at room temperature in the place with little light. Slides were once more cleaned on three separate occasions in PBS following incubation. For five minutes, the nuclei were counterstained with DAPI (1 μg/mL in PBS)., and then a final PBS wash was performed. The sections were coverslipped after being mounted with an anti-fade mounting medium. Sections were imaged using a Zeiss LSM 880 confocal microscope at 40 × magnification. Fluorescence intensity was quantified using ImageJ software 6.0 (MD, USA). Negative controls omitting primary antibodies confirmed specificity.

Measurement of inflammatory factors

Sterile enzyme-free tubes were used to collect liver and cecal samples. ELISA, a commercial kit, was employed to measure the contents of LPS (DL233211O1), ROS (DL445519O1), DAO (DL987634O1), IL-1β (DL661233O1), IL-18 (393412O1), TNF-α (DL651233O1), and IL-10 (DL466623O1) (Jiangsu Meimian industrial Co., Ltd China).

Serum biochemistry

Whole blood was collected, allowed to clot for ~30 min at room temperature, and centrifuged at 1,500 × *g* for 10 min at 4°C to obtain serum. Serum was aliquoted to avoid repeated freeze thaw cycles and stored at −20°C until analysis. Serum concentrations of total cholesterol (T-CHO, cat. B111-1-1), low-density lipoprotein cholesterol (LDL-C, A11-1-5), high-density lipoprotein cholesterol (HDL-C, B131-1-1), triglycerides (TG, 127-1-1), blood urea nitrogen (BUN, K-121-1-5), glucose (GLU, E111-1-1), and lactate (F112-9-8) were measured using enzymatic colorimetric kits supplied by Shanghai Mlbio Biotechnology Co., Ltd. (China). Serum aspartate aminotransferase (AST) and alanine aminotransferase (ALT) activities were quantified with a Roche automated biochemical analyzer (Roche Diagnostic System Inc., Indianapolis, IN, USA) using kits from Nanjing Jiancheng Bioengineering Institute (China). Liver samples were snap-frozen in liquid nitrogen, stored at −80°C, and homogenized in ice-cold buffer according to the manufacturer's instructions. Hepatic concentrations of T-CHO (B111-1-1), LDL-C (A11-1-5), HDL-C (B131-1-1), TG (127-1-1), and glycogen (B-101-9-1) were determined with commercial kits from Shanghai Mlbio Biotechnology Co., Ltd. (China). To confirm assay applicability to goose serum, we assessed (i) parallelism between serial dilutions of pooled goose serum and kit standard curves; (ii) dilution linearity ($r \geq 0.99$); (iii) spike-and-recovery of standards added to goose serum (90–110 % acceptable range); and (iv) precision, with intra-assay and inter-assay coefficients of variation ≤10 % and ≤15 %, respectively.

Determination of immunoglobulins

Commercial enzyme-linked immunosorbent assay (ELISA) kits (Meimian Industrial Co., Ltd., Jiangsu, China) were used to measure the serum concentrations of immunoglobulin A (IgA), immunoglobulin G (IgG), and immunoglobulin M (IgM). Every assay was carried out in compliance with the procedures outlined by (Chen et al., 2021).

Analyses of H_2O_2 and $O^{\bullet 2-}$

Hepatic superoxide anion (O_2^-) levels were measured using a chemiluminescence assay. Briefly, liver tissues were homogenized in lysis buffer (pH 7.4) containing 20 mM HEPES and 10 mM EDTA. After centrifugation at 1000 × g for 10 min, Krebs-HEPES buffer with pH 7.4, containing 5 mM lucigenin (Sigma, Shanghai, China) was added to aliquots, and they were incubated for two minutes at 37°C. Chemiluminescence was recorded using a multifunctional microplate reader (M200 PRO, TECAN, Switzerland), and mean light units (MLU) per minute per milligram of protein were used to express the results. Superoxide dismutase was added to validate superoxide specificity. (SOD; 350 U/mL; R&D Systems, Minneapolis, MN, USA).

Liver tissues were homogenized in normal saline and treated with a similar amount of cold methanol at 4°C for 60 min to measure the level of hydrogen peroxide (H_2O_2). After centrifuging the samples for 30 min at 10,000 × *g*, the supernatant was utilized to quantify H_2O_2 using commercial assay kits. Bovine serum albumin (BSA) was used as the standard in the Bradford method to measure protein concentrations.

Measurement of antioxidant activity

The catalase (CAT), superoxide dismutase (SOD), and glutathione

peroxidase (GSH-Px) enzyme activities were determined calorimetrically. Liver and ceca total antioxidant capacity (T-AOC), TBAR (thiobarbituric acid reactive substances), and malondialdehyde (MDA) levels were determined by commercial assay kits provided by Seamaty Technology Co., Ltd. Chengdu, China.

Morphological analysis of ileum and ceca

Fixed ileum tissues were dehydrated through a graded ethanol series and embedded in paraffin. Tissue sections were prepared and stained with hematoxylin and eosin (H&E) following Standardized procedures (Wuhan Servicebio Technology Co., Ltd., Wuhan, China). For goblet cell analysis, Periodic acid-Schiff (PAS) staining was applied to cecal tissue sections, which were then seen at 40 × magnification using an optical microscope. In every visible field, goblet cells (purple-stained) and neutral mucins were located, measured, and assessed for morphological traits.

Liver histopathology

After being preserved for 24 h in 4 % paraformaldehyde, liver tissues were dehydrated using a series of graded ethanol and paraffin embedding. . Paraffin-embedded samples were sectioned at 5 μm thickness and stained with hematoxylin and eosin (H&E) for histological evaluation. Morphological analysis including liver pathology score, hepatocyte necrosis, Ishaq fibrosis score, hepatocyte size, apoptotic bodies, inflammatory cell count and sinusoidal dilation was performed using a digital microscope (Olympus BX51, Tokyo, Japan).

Gene expression assays

Total RNA was extracted from pulverized cecal tissue and tibia using TRIzol reagent (Invitrogen, Carlsbad, CA, USA) following the manufacturer's protocol. RNA quality was assessed by spectrophotometry (NanoDrop, Thermo Fisher Scientific, USA), and only samples with an A260/A280 ratio of 1.8–2.0, an A260/A230 ratio > 1.8, and clear 28S and 18S rRNA bands (≈2:1) on agarose gel were used for downstream analysis. One microgram of RNA was reverse-transcribed into cDNA using the Evo M-MLV RT Kit (cat. no. AG11706, Accurate Biotechnology, Hunan, China). Quantitative real-time PCR (qPCR) was carried out on a QuantStudio 5 Real-Time PCR System (Applied Biosystems, Thermo Fisher Scientific, Waltham, MA, USA) using SRBR Green Premix Pro Taq HS qPCR kit, (AG11701, ACCURATE BIOTECHNOLOGY, HUNAN) under the following cycling conditions: initial denaturation at 95°C for 10 min, followed by 40 cycles of 95°C for 2 s and 60°C for 1 min. A melting curve analysis (95°C for 15 s, 65°C for 1 min, and 95°C for 15 s) was performed to verify amplification specificity. Primers for all target genes were designed with Primer3 software (sequences listed in Supplementary Table 1), and relative expression was calculated using the ΔΔCt method, normalized against two housekeeping genes, GAPDH and β-actin. Primer specificity and amplification efficiency (90–110 %) were confirmed using standard curves generated from serially diluted cDNA. Each gene was analyzed using three biological replicates per sample, and each reaction was run in technical triplicate to ensure reproducibility.

Western blotting

A liver sample of around 0.3 g was lysed in 3 mL of lysis buffer after being ground in liquid nitrogen. A bicinchoninic acid (BCA) protein assay kit (Thermo Fisher Scientific Inc., USA) was used to measure the protein concentration in the supernatant after centrifugation. Using the Trans-Blot Turbo Transfer System (Bio-Rad, USA), equal volumes of protein lysates were separated on 10 % SDS-polyacrylamide gels (SDS-PAGE) and then moved onto polyvinylidene difluoride (PVDF) membranes. Following a one-hour blocking period of the membranes at 25°C in 5 % non-fat milk in Tris-buffered saline with 0.1 % Tween-20 (TBST), the following primary antibodies were incubated overnight at 4°C: FAS (Abclonal, C3212), PPARα (Abclonal, A4141), NrF2 (Abcam, ab1915), Keap-1 (Abcam, B4617), NLRP3 (Abcam 1725), Caspase-3 (Proteinintech, GR2212-63), TLR-4 (Huaxingbio, 3254), NF-κB p65 (ab1703-19), and GAPDH (Abclonal, LA033). Using a chemiluminescent substrate (such as ECL), immunoreactive bands were found and measured using densitometry. Protein expression levels have been standardized using GAPDH as a loading control.

NrF2 and NF-κB immunofluorescence (IF) imaging

Liver tissue slices were fixed in 4 % paraformaldehyde for 10 min, dewaxed in xylene for 15 min, and rehydrated through graded alcohol to distilled water. Antigen retrieval was performed using citrate buffer (pH 6.0) under high temperature and pressure in a pressure cooker; after the cooker reached pressure, tissues were heated for 2 min and then cooled to room temperature. For weakly expressed targets, EDTA buffer (pH 9.0) was alternatively used. Following retrieval, sections were blocked with 10 % fetal bovine serum for 30 min and incubated overnight at 4°C with primary antibodies against NF-κB (Abways, CY2329, 1:200) and Nrf2 (PTG, 67201-IG, 1:200). Detection was performed using HRP Goat Anti-Rabbit IgG (1:400, 50 min, RT, dark), followed by tyramide signal amplification with tyramine sodium fluorescein (Servicebio, G2150-1 L) in PBST containing 0.0003 % H_2O_2 for 20 min at room temperature. Nuclei were counterstained with DAPI (10 min, RT), mounted with antifade medium (Servicebio, G1401, Fluoroshield with DAPI). Confocal images were acquired on a Leica TCS SP8 STED confocal microscope with a magnification of 20X. Fluorescein signals were excited with a laser and detected using a 586 nm emission window. DAPI was excited with a 586 nm laser. Fluorescence intensity was quantified using ImageJ 6.0 (MD, USA) by converting the fluorescence image into a grayscale image, and the cumulative fluorescence intensity value (IntDen) and corresponding positive pixel area of each slice respectively with pixel as a standard unit. The average fluorescence intensity was calculated as IntDen/Area and results were obtained from three different images.

Statistical analysis

One-way analysis of variance (ANOVA) was used in SPSS software version 27.0 (IBM Corp., Armonk, NY, USA) for statistical analysis after the Shapiro-Wilk test ($W > 0.05$) confirmed that the data was normally distributed. The least significant difference (LSD) test was used for post hoc multiple comparisons where significant differences were found. All figures provide the data as means ± standard deviation (SD). The following criteria were used to signify statistical significance: $^{*}p < 0.05$ and $^{**}p < 0.01$.

Results

Growth performance

The feed conversion ratio (FCR) exhibited a significant decline as a result of a notable drop in feed intake and average daily growth compared to the control group. Zn_Gly supplementation reversed this trend which was depicted on Fig. 1 (a-c). However, the LPS + Zn_Gly group and the CON group differed significantly ($p < 0.05$). LPS administration significantly increased ($p < 0.05$) the liver index, while zinc glycine reduced this normal levels observed in CON group (Fig. 1d).

Effect of Zn_Gly on systemic inflammatory factors

Compared with CON group, LPS content in liver and ceca was significantly increased in geese challenged with LPS. Zn_Gly supplementation significantly reversed ($p < 0.01$) the LPS content both in liver and ceca in the geese (Fig. 1e-f). Similar trend was found in case of ROS

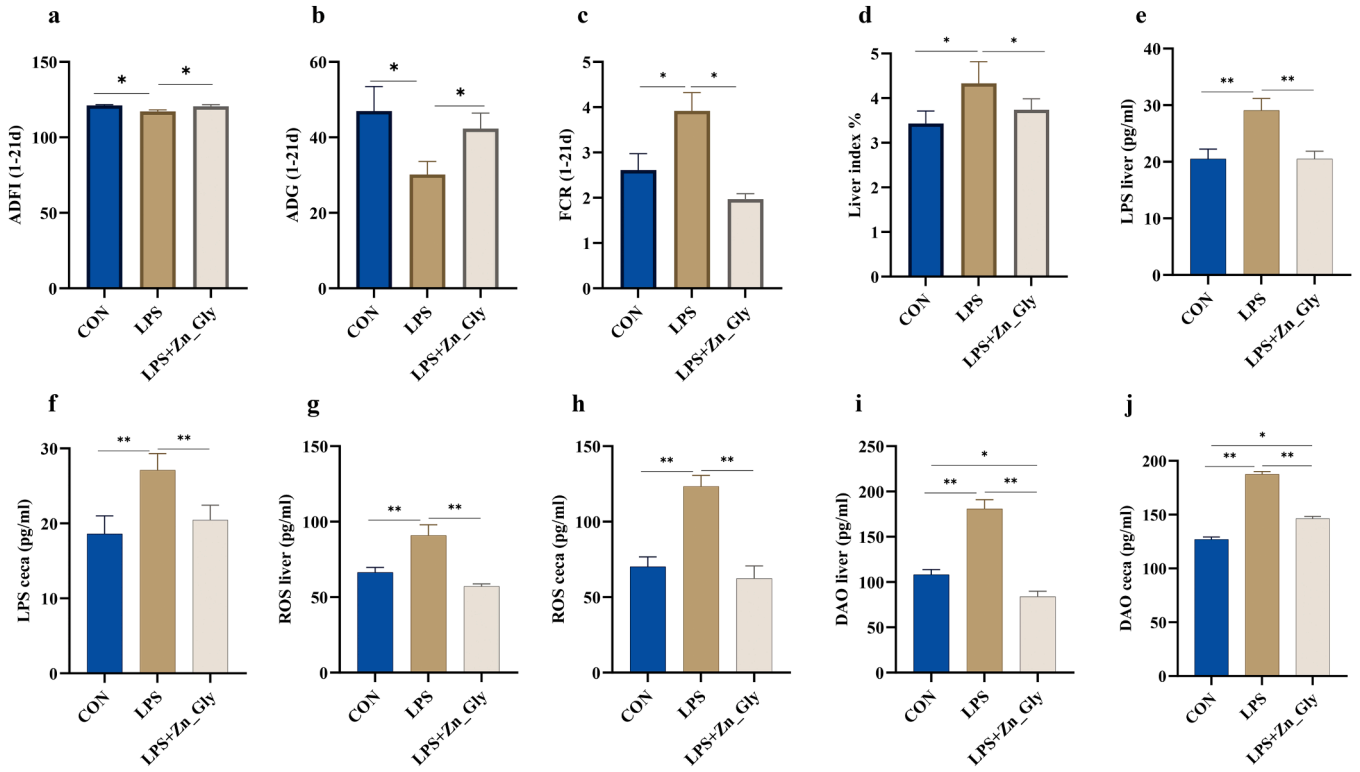

Fig. 1. Effects of Zn_Gly on growth performance and systemic inflammation. (a-d) ADFI, ADG, FCR and liver index. (e-j) LPS, ROS, DAO content in liver and ceca of geese. The asterisks symbol indicates significant differences $*p < 0.05$, $**p < 0.01$. (ADFI: average daily feed intake; ADG: average daily gain; FCR: feed conversion ratio; LPS: lipopolysaccharide; ROS: reactive oxygen species; DAO: diamine oxidase.

as a result of Zn_Gly supplementation (Fig. 1g-h). Diamine oxidase (DAO) levels were significantly affected by treatments in both liver and ceca. In the liver, the LPS group showed markedly elevated DAO levels compared to the LPS+ Zn_Gly group and CON group (Fig. 1i). Similarly, the LPS group had significantly greater ($p < 0.01$) DAO levels of the ceca in contrast to the LPS+ Zn_Gly and CON groups (Fig. 1j). However, there was also significant difference in liver DAO levels between CON and Zn_Gly groups. These results indicated that LPS administration increased intestinal permeability, as reflected by elevated LPS, ROS and DAO levels, and that Zn_Gly supplementation potentially mitigated this effect.

Zn Gly improved serum and liver metabolic profile

LPS administration considerably raised ($p < 0.01$) serum T-CHOL, TG and LDL concentrations as compared to CON group. Zn_Gly supplementation reduced the elevated serum concentrations of T-CHOL, triglycerides, and LDL caused by LPS to levels seen in the CON group (Supplementary Fig. 1 a-c). Serum blood urea nitrogen and glucose (GLU) concentrations were significantly increased in LPS group, while zinc glycine supplementation reversed this effect (Supplementary Fig. 1 d-e). However, both CON and Zn_Gly also showed significant difference in serum BUN concentration. Zinc glycine significantly improved the serum HDL concentration to the levels observed in CON group when compared to LPS group (Supplementary Fig. 1 f). Similar trend was observed in liver in terms of lipid biochemistry profile (Supplementary Fig. 1 g-l).

Zn Gly improved the antioxidant status in geese

Antioxidant status was affected as a result of LPS challenge. Malondialdehyde (MDA) and TBAR (thiobarbituric acid reactive substances) amount in liver were markedly increased in LPS group compared to the CON group. Zn_Gly supplementation notably reversed the effects of LPS by reversing the levels of TBAR and MDA being observed in CON group (Fig. 2a and b). Superoxide dismutase (SOD), glutathione peroxidase (GSH-PX) and catalase (CAT) and are crucial in improving the antioxidant defense mechanism compromised due to inflammation. Zn_Gly supplementation greatly elevated ($p < 0.01$) these enzymes in liver than to LPS group (Fig. 2c-e). LPS administration significantly decreased total antioxidant capacity (T-AOC) compared to the controlled group, whereas Zn_Gly supplementation effectively restored T-AOC levels to those comparable with controls (Fig. 2f). Zn_Gly significantly downregulated the mRNA expression of MDA in the liver as compared to LPS group. The CON and LPS + Zn_Gly groups did, however, differ significantly as well (Fig. 2g). LPS significantly downregulated the mRNA expression levels of CAT and SOD, while dietary zinc glycine reversed this and upregulated CAT and SOD expression in the liver (Fig. 2h-i). We observed the similar trends in terms of MDA and TBAR in the ceca but Zn_Gly reduced these levels more significantly ($p < 0.05$) than CON group (Supplementary Fig. 2 a-b). Zn_Gly supplementation exhibited a significant increase in SOD, GSH-PX and CAT enzymes in liver as compared to LPS group (Supplementary Fig. 2 c-e). Similar trend was found in terms of ceca T-AOC levels. However, there was also a significant difference between CON and LPS + Zn_Gly group (Supplementary Fig. 2 f). Zn_Gly substantially downregulated MDA mRNA expression in the ceca as compared to LPS group also (Supplementary Fig. 2 g). Dietary Zn_Gly appreciably upregulated the gene expression of CAT and SOD in the ceca demonstrating its role in antioxidant defense mechanism (Supplementary Fig. 2 h-i).

Zn Gly mitigated the adverse effects of inflammatory cytokines favoring liver recovery

Inflammatory cytokines play a crucial role in liver injury under ongoing inflammatory reactions. Geese under LPS challenge stress had significantly increased the level of IL-1β both in liver and ceca (gut–liver

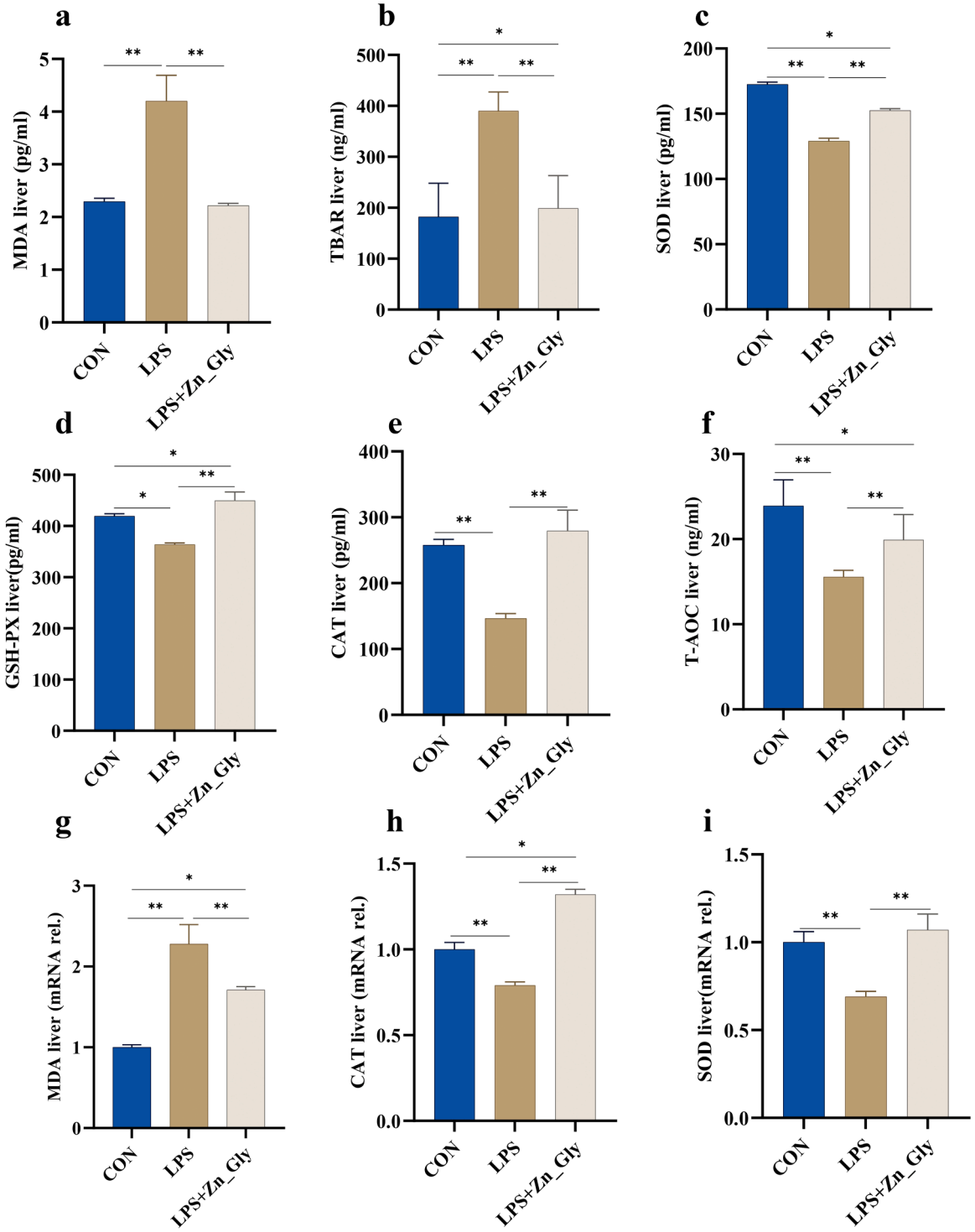

Fig. 2. Effects of Zn_Gly on antioxidant status in liver. (a-f) MDA, TBAR, SOD, GSH-PX, CAT and T-AOC. (g-i) mRNA expression of MDA, CAT and SOD in liver. The asterisks symbol indicates significant differences $*p < 0.05$, $**p < 0.01$. (MDA: malondialdehyde; TBAR: thiobarbituric acid reactive substances; SOD: superoxide dismutase, GSH-PX: glutathione peroxidase; CAT: catalase; T-AOC: total antioxidant capacity.

axis). Supplementation of Zn_Gly significantly restored the adverse of LPS by reducing the IL-1β levels both in liver (Fig. 3a). Zn_Gly was very effective in reducing the IL-18 levels as compared to LPS group, however this effect was higher as compared to CON group (Fig. 3b). TNF-α level in liver was notably greater ($p < 0.01$) and Zn_Gly helped in lowering such levels (Fig. 3c). IL-18 also known as pro-inflammatory cytokine, was also measured from liver and ceca to determine its effect in promoting health gut–liver axis. LPS administration significantly reduced ($p < 0.01$) reduced the levels of IL-10 in liver and Zn_Gly effectively restored the IL-10 levels (Fig. 3d). In addition, LPS + Zn_Gly group showed better effect than CON group. In the cecal contents, we observed the similar trends in case of IL-1β as observed in the ceca (Fig. 3e). LPS challenge significantly increased the cecal IL-18 levels, while Zn_Gly significantly reversed this effect but this effect was lower in comparison with CON group (Fig. 3f). For TNF-α level in ceca, dietary Zn_Gly significantly reduced ($p < 0.05$) with respect to LPS group. However,

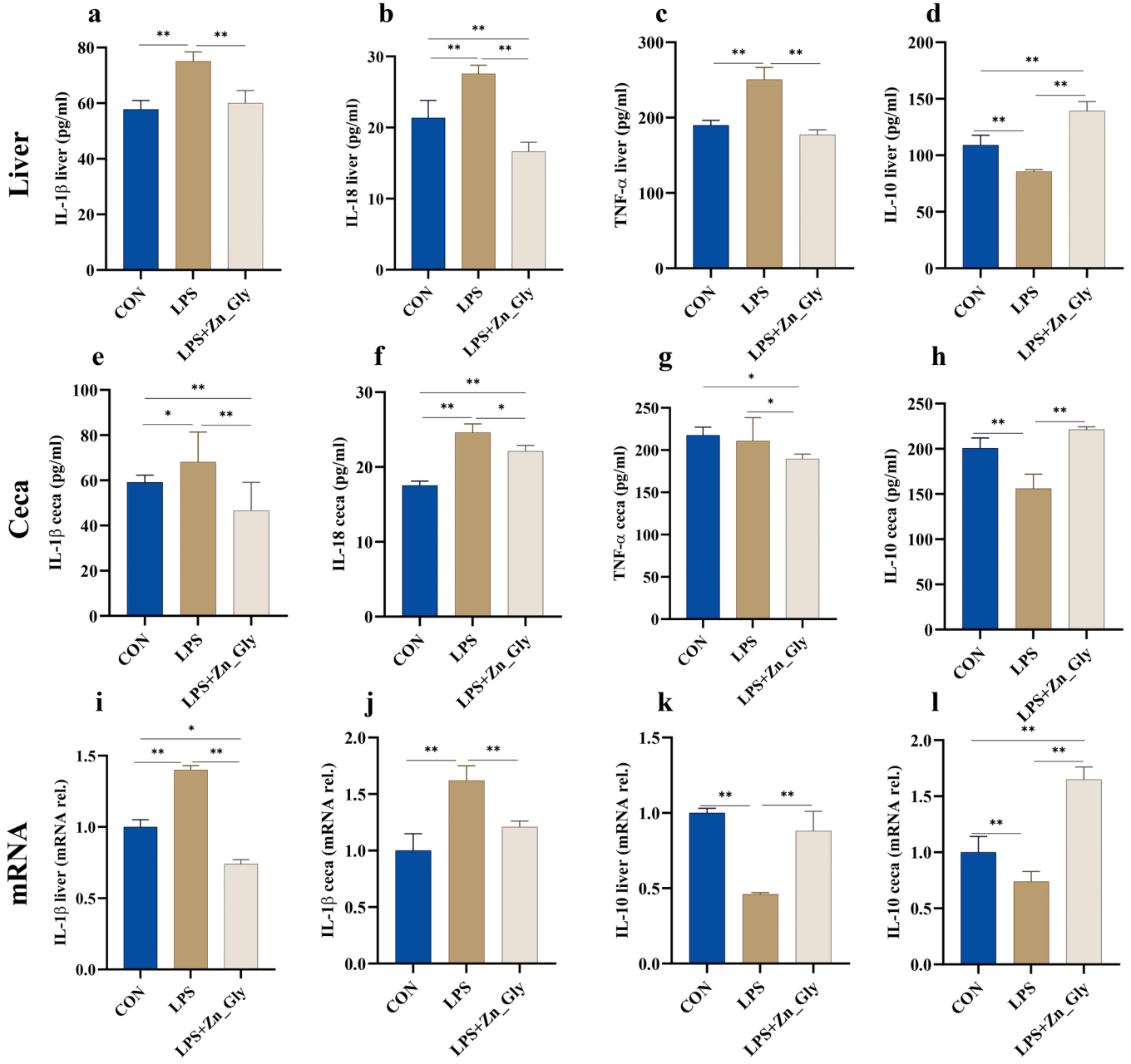

Fig. 3. Effects of Zn_Gly on inflammatory and anti-inflammatory cytokines in liver and ceca. (a-d) IL-1β, IL-18, TNF-α and IL-10 concentration in liver. (e-h) IL-1β, IL-18, TNF-α and IL-10 concentration in ceca. (i) mRNA expression of IL-1β in liver. (j) mRNA expression of IL-1β in ceca. (k) mRNA expression of IL-10 in liver. (l) mRNA expression of IL-10 in ceca. The asterisks symbol indicates significant differences $*p < 0.05$, $**p < 0.01$. (IL: interleukin; TNF-α: tumor necrosis factor-α).

this impact of Zn_Gly was higher compared to CON group (Fig. 3g). LPS administration significantly reduced ($p < 0.01$) reduced the levels of IL-10 in ceca and Zn_Gly effectively restored the IL-10 levels (Fig. 3h). Gene expression results showed that Zn_Gly dramatically dropped ($p < 0.01$) the IL-1β levels both in liver and ceca by upregulating the gene expression of IL-10 (Fig. 3i-l).

Effect of Zn Gly on liver histopathology of geese with LPS induced liver injury

H&E staining was performed to evaluate the histological parameters related to liver injury under LPS challenge (Fig. 4a). LPS administration significantly increased ($p < 0.01$) the liver pathology score, which was reversed as a result of dietary Zn_Gly. However, there was also a significant difference between CON and LPS + Zn_Gly (Fig. 4b). Zn_Gly significantly reduced the hepatocyte necrosis area, Ishaq fibrosis, hepatocyte size and apoptotic bodies score as compared to LPS group (Fig. 4c-f). However, there was also a significant difference between CON and LPS + Zn_Gly group regarding these parameters. Zn_Gly significantly decreased the inflammatory cell count and sinusoidal dilation to the levels observed in CON group as compared to LPS group (Fig. 4g-h). An important factor in chronic liver damage is liver enzyme. Zn_Gly reduced the AST and ALT amount contrasting to LPS group (Fig. 4i-j). In addition, there was also a notable distinction in terms of ALT level between CON and LPS + Zn_Gly groups. LPS challenge significantly elevated the levels of IgG as compared to CON and LPS + Zn_Gly group. Zn_Gly reversed this effect (Fig. 4k). Zinc glycine elevated the quantity of IgM and IgA as compared to LPS group (Fig. 4 l-m). However, this effect was lower than compared to CON group. Regarding liver H_20_2, $O^{\cdot 2}$ and NO activity, Zn_Gly significantly reduced ($p < 0.01$)

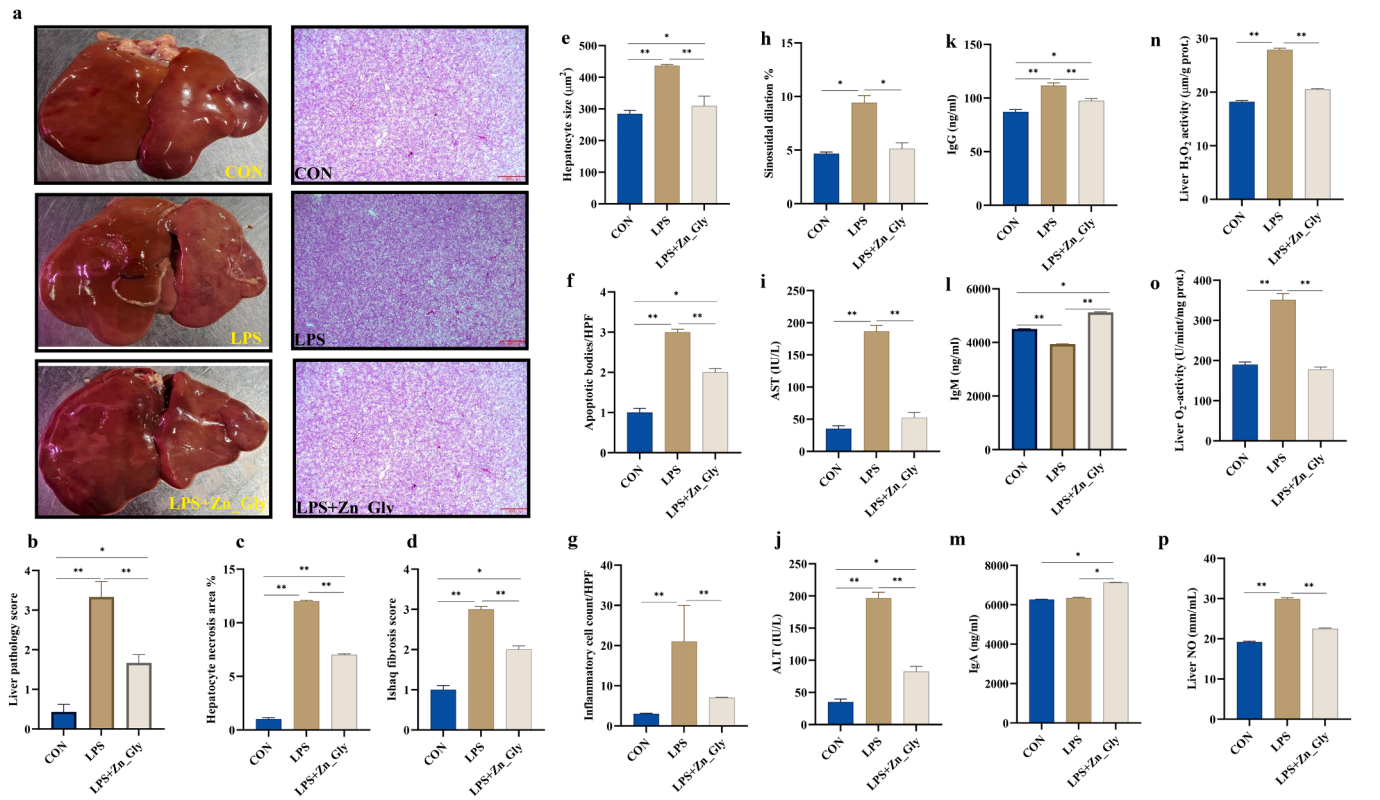

Fig. 4. Effects of Zn_Gly on liver histopathology of LPS induced gut-liver inflammation. (a) liver images and H&E. (b-h) liver pathology score, hepatocyte necrosis area, Ishaq fibrosis score, hepatocyte size, apoptotic bodies, inflammatory cell count and sinusoidal dilation. (i-j) AST and ALT. (k-m) IgG, IgM and IgA. (n-p) liver H_2O2, $O^{\cdot 2}$ and NO activity. The asterisks symbol indicates significant differences $*p < 0.05$, $**p < 0.01$. (ALT: aspartate aminotransferase; AST: aspartate aminotransferase).

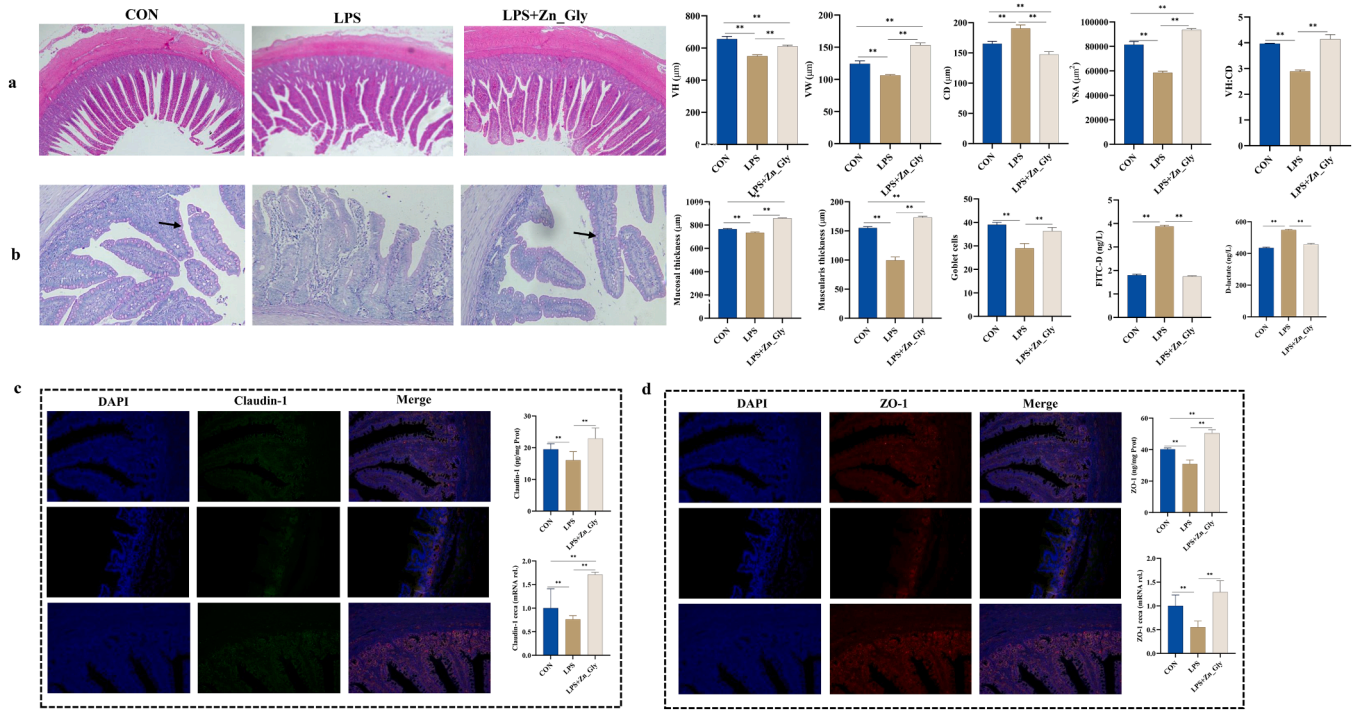

Fig. 5. Effects of Zn_Gly on intestinal morphology of geese with LPS induced inflammation. (a) ileum H&E representing VH, VW, CD, VSA and VH:CD. (b) AB-PAS stain representing mucosal thickness, muscularis thickness, goblet cells, FITC-D and D-lactate. (c) Protein expression of ZO-1 through immunofluorescence and its mRNA expression in ceca. (d) protein expression of claudin-1 through immunofluorescence and its mRNA expression in ceca. The asterisks symbol indicates significant differences $*p < 0.05$, $**p < 0.01$. (VH: villus height; VW: villus width; CD: crypt depth; VSA: villus surface area; VH:CD: villus height to crypt depth ratio; FITC-D: fluorescently-labelled small molecule-dextran, ZO-1: zonula-1).

these parameters to the CON group's observed levels as compared to LPS treated group (Fig. 4n-p).

Effect of Zn Gly on intestinal morphology of geese with LPS induced intestinal inflammation

Gut morphology was significantly impacted by LPS and LPS + Zn_Gly, according to intestinal H&E staining of the ileum and ceca. Fig. 5a represented the ileum morphology. Zn_Gly increased the villus height (VH), villus width (VW) significantly ($p < 0.01$) as compared to LPS group (Fig. 5a). LPS administration significantly increased the crypt depth (CD) which was restored to normal as a result of dietary zinc glycine addition. However, Zn_Gly showed better effect than CON group. Villus surface area (VSA) and villus height to crypt depth ratio (VH: CD) was improved ($p < 0.01$) as a result of Zn_Gly supplementation as compared to LPS group. Fig. 5b represented the cecal Ab-PAS stain. Zn_Gly supplementation also resulted in increased ($p < 0.01$) ceca mucosal and muscularis thickness. Geese challenged with LPS had lower number of goblet cells, while Zn_Gly restored the goblet cells to the level observed in CON group (Fig. 5b)

Effect of Zn Gly on intestinal barrier function in geese LPS induced inflammation

Intestinal permeability

Compared to the CON group, the LPS group's serum FITC-D and D-LA

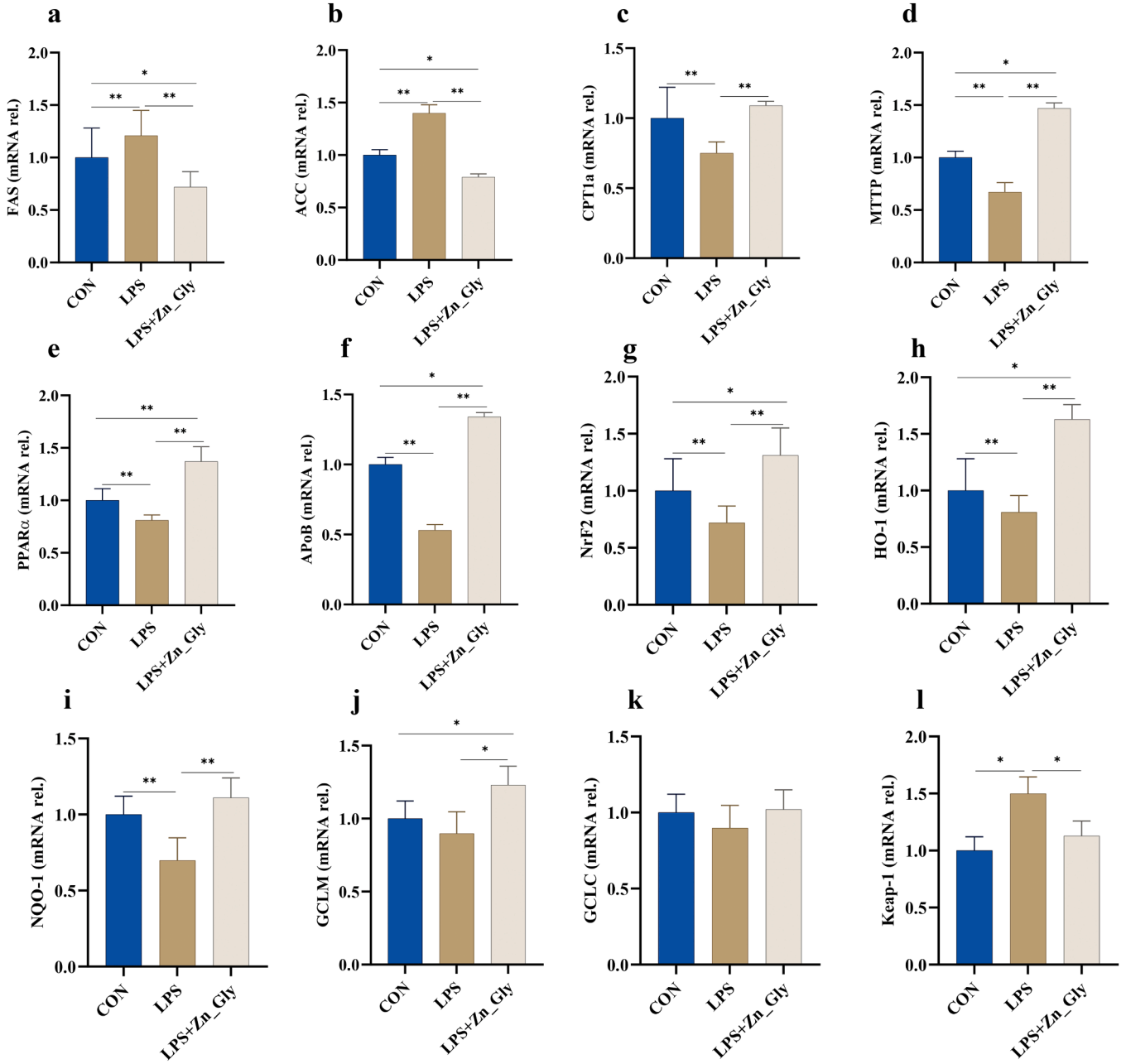

Fig. 6. Effects of Zn_Gly on gene expression of β-oxidation and antioxidant genes in the liver of geese. (a-f) gene expression of FAS, ACC, CPT-1a, MTTP, PPARα and APoB. (g-l) gene expression of NrF2, HO-1, NQO-1, GCLM, GCLC and Keap-1. The asterisks symbol indicates significant differences $*p < 0.05$, $**p < 0.01$. (FAS: fatty Acid synthase; ACC: acetyl-CoA carboxylase CPT1a: carnitine palmitoyltransferase 1A; MTTP: microsomal triglyceride transfer protein; PPARα: peroxisome proliferator-activated receptor alpha; APoB: apolipoprotein B; NrF2: nuclear factor erythroid-derived like 2; HO-1: heme oxygenase 1; NQO-1: NAD(P)H quinone dehydrogenase 1; GCLM: glumate-cysteine ligase modifier subunit; GCLC: glumate-cysteine ligase catalytic subunit; Keap-1: kelch-like ECH-associated protein 1.

levels were found considerably greater (Fig. 5b). However, Zn_Gly significantly reduced both of the levels. Therefore, by regulating intestinal permeability, Zn_Gly may contribute to the maintenance of intestinal barrier function.

Physical barrier

Tight junction (TJ) proteins, including ZO-1 and claudin-1 play a critical role in maintaining gut integrity. Immunofluorescence analysis of ceca showed that in the LPS challenge group, levels *ZO-1* and *CLDN-1* was significantly altered (Fig. 5c-d). LPS treatment markedly reduced ZO-1 protein and mRNA expression levels, while Zn_Gly supplementation significantly upregulated ($p < 0.01$) protein and mRNA expression levels of ZO-1 (Fig. 5c) and claudin-1 protein expression ($p < 0.05$). Furthermore, *claudin-1* protein and mRNA levels were remarkably increased as a result of Zn_Gly supplementation (Fig. 5d).

Zn_Gly alleviated LPS-induced liver damage through key signaling genes

β-oxidation plays a protective role by breaking down excess fatty acids, thereby preventing lipid accumulation and steatosis. LPS challenge significantly upregulated ($p < 0.01$) the gene expression of Fatty Acid Synthase (FAS) and Acetyl-CoA Carboxylase (ACC) reducing the β-oxidation process. Oral supplementation of zinc glycine (Zn_Gly) had been shown to reverse this effect by downregulating the expression these genes (Fig. 6a-b). Zn_Gly upregulated the mRNA expression levels of Carnitine Palmitoyltransferase 1A (CPT1a), Microsomal Triglyceride Transfer Protein (MTTP), Peroxisome Proliferator-Activated Receptor Alpha (PPARα) and Apolipoprotein B (APoB) as shown in the Fig. 6c-f. However, Zn_Gly showed better effect than CON group. Proper β-oxidation also reduces oxidative stress along with limits the generation of pro-inflammatory lipid mediators. LPS challenge significantly upregulated the gene expression of Keap-1 as compared to CON and LPS + Zn_Gly groups. Zn_Gly significantly downregulated this gene expression by upregulating the NrF2 and its regulating genes namely Heme Oxygenase-1 (HO-1), NADPH Quinone Dehydrogenase 1 (NQO-1), Glutamate-Cysteine Ligase Modifier Subunit (GCLM). However, Regarding the Glutamate-Cysteine Ligase Catalytic Subunit (GCLC), no discernible variation was observed among the groups. Gene expression data of antioxidant defense mechanism was shown in the Fig. 6g-l. In LPS-induced liver injury, the inflammatory response is primarily mediated through the activation of the NF-κB pathway. Geese under LPS challenge had significant high gene expression of NLRP3, TLR-4, MyD88, TRAF-6, IKKα, Rela leading to increased activation of NF-κB. These genes were significantly downregulated as a result of dietary Zn_Gly as compared to LPS group (Supplementary Fig. 3 a-g). Western blot analysis provided additional confirmation that Zn_Gly decreased the protein expression of FAS by increasing the protein expression of PPARα (Fig. 7A-B). Regarding antioxidant defense mechanism NrF2-Keap-1 (key pathway), Zn_Gly significantly increased protein expression of NrF2 by reducing Keap-1 protein levels (Fig. 7C-D). NLRP3, IKKα and MyD88 were also decreased as a result of dietary zinc glycine (Fig. 7E-G). Regarding the inflammatory pathway (TLR-4- NF-κB), Zn_Gly significantly reduced the protein expression the TLR-4 and NF-κB (Fig. 7H-I).

Immunofluorescence (IF) exploration of NF-κB and NrF2 localization in liver

Immunofluorescence investigation was used to evaluate the nuclear translocation of meat geese in order to confirm the NF-κB triggering and signaling of Nrf2 in the liver. In contrast to the CON and LPS + Zn_Gly groups, confocal fluorescence microscopy showed that NF-κB was more prominently located in the cell nuclei of tissue in liver in the LPS group (Fig. 8a). Furthermore, the nuclear translocation of NrF2 was examined using immunofluorescence to examine the impact of zinc glycine on the live protection pathway. This analysis revealed that NrF2 was intracellularly distributed and expressed at a higher level in the LPS + Zn_Gly group than in the LPS group (Fig. 8b). The findings showed that the

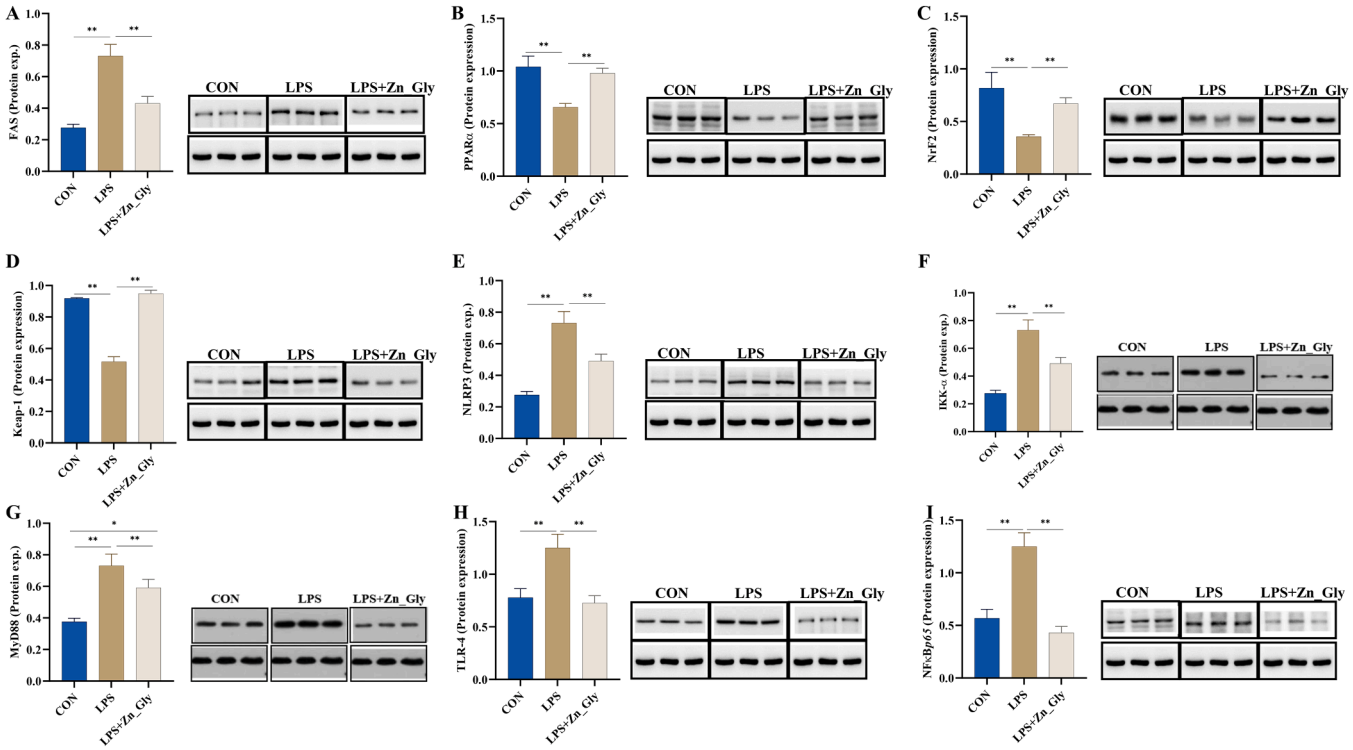

Fig. 7. Effects of Zn_Gly on protein expression of β-oxidation, antioxidant genes, apoptotic genes and inflammatory pathway NFκB and its genes in the liver of geese. (a-h) protein expression of FAS, PPARα, NrF2, Keap-1, NLRP3, IKKα, MyD88, TLR-4 and NFκB*p65*. The asterisks symbol indicates significant differences $*p < 0.05$, $**p < 0.01$.

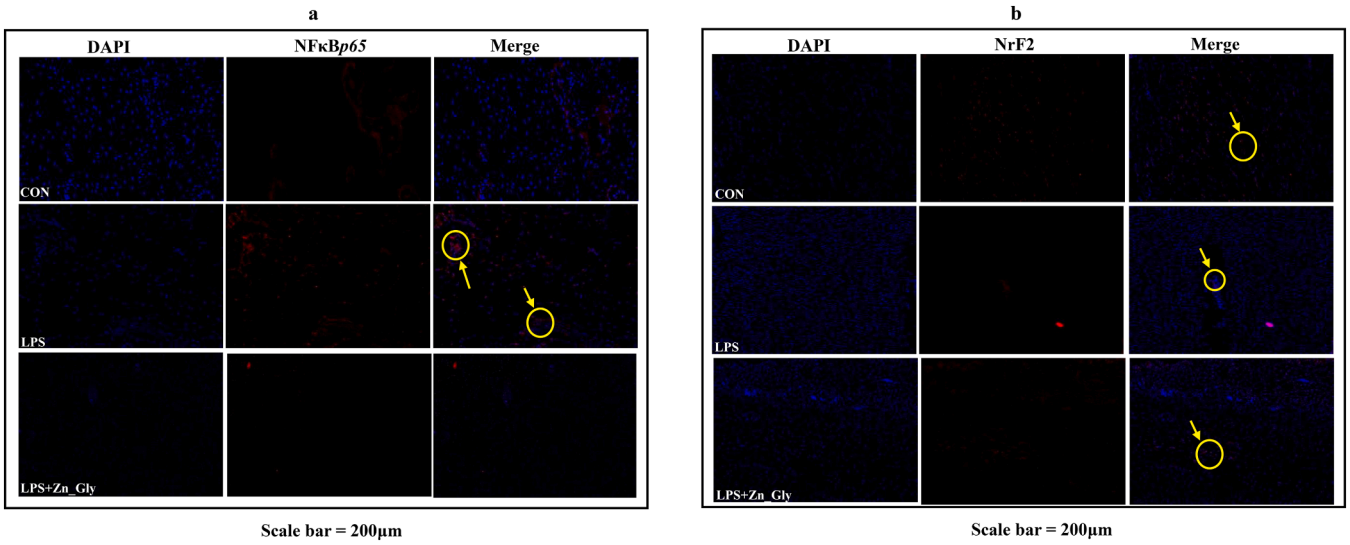

Fig. 8. Effects of Zn_Gly on NFκB*p65*/NrF2 signaling in liver of geese. (a) Immunofluorescence (IF) of NFκB. Rabbit Anti- NFκB (1:500/1:200) showing nuclear translocation of NFκB. Blue: nucleus (DAPI); Red: NFκB staining; Merge; combination of blue and red indicating nuclear translocation of NFκB, scale bar = 200um. (b) Immunofluorescence (IF) analysis using Rabbit NrF2 (1:500/1:200) showing nuclear translocation of NrF2 in the tibia of meat geese. Blue: nucleus (DAPI); Red: NrF2 staining; Merge; combination of blue and red indicating nuclear translocation of NrF2, scale bar = 200um. (NFκB: nuclear factor kappa beta; NrF2: NrF2: nuclear factor erythroid-derived like 2). Arrows and circles represented the expresssions of NFκB and NrF2.(For interpretation of the references to color in this figure legend, the reader is referred to the web version of this article.).

Zn_Gly group had higher NrF2 than the LPS group, indicating that dietary Zn_Gly may actively prevent LPS-induced liver damage in geese.

Discussion

This research offers strong proof that dietary supplementation with zinc glycine (Zn_Gly) effectively mitigates lipopolysaccharide (LPS)-induced liver damage in geese, primarily by modulating the Nrf2 and NF-κB signaling pathways. The gut-liver axis, a critical interface for immune and metabolic homeostasis, is highly susceptible to endotoxin-driven inflammation, especially in avian species with metabolically active livers like geese. Our findings highlight Zn_Gly as a potential therapeutic nutritional strategy to restore hepatic and intestinal integrity under inflammatory challenge (Fig. 9).

LPS administration led to a significant reduction in feed intake and ADG, alongside an increased feed conversion ratio (FCR), indicating a

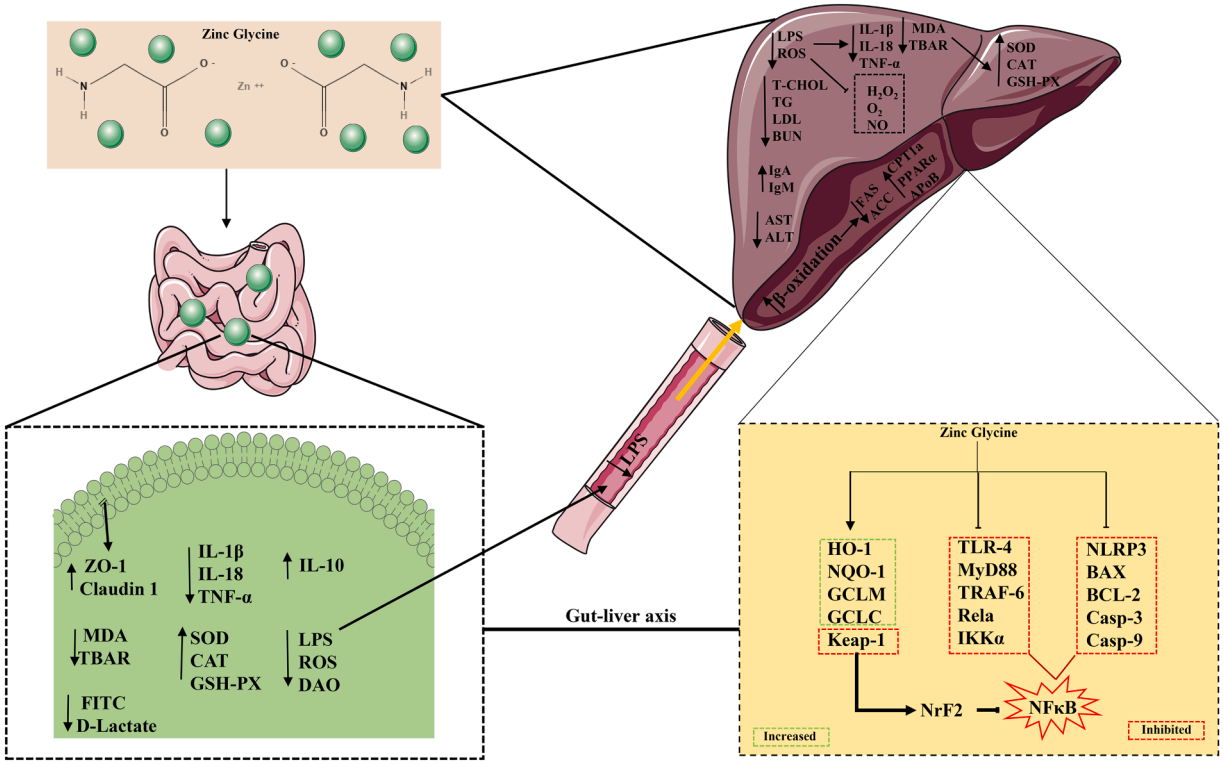

Fig. 9. Schematic diagram of Zn_Gly alleviating LPS-induced hepatic damage through regulating NFκB/NrF2 signaling in geese.

typical systemic response to endotoxemia (LPS) and metabolic stress. This alteration in growth performance highlights the impact of LPS-induced inflammation, which can disrupt normal metabolic processes. As a consequence, these physiological changes are often accompanied by increased oxidative stress, which exacerbates tissue damage and further impairs growth. In the present study, we observed an elevation in markers of oxidative stress, which correlates with the metabolic disturbances noted in the growth performance data (Ma et al., 2011). These findings suggest that the decline in feed intake and ADG could, in part, be attributed to the oxidative burden imposed by endotoxemia. Zn_Gly supplementation ameliorated these changes, although not entirely restoring performance to control levels, suggesting a protective but not entirely restorative role. These results align with earlier research that demonstrated zinc's involvement in nutrient metabolism and growth regulation under stress conditions (Abuajamieh et al., 2020).

The anti-inflammatory potential of organic zinc sources has been increasingly recognized, with effects on intestinal health, tissue zinc deposition, antioxidant defense, and immune regulation (Jarosz et al., 2017, 2019; Zhang et al., 2018; Chand et al., 2021). Our findings align with previous studies showing that zinc supplementation enhances immune balance by modulating Th1/Th2 responses and reducing cytokine-driven intestinal damage (Xie et al., 2021). Zn_Gly administration suppressed pro-inflammatory cytokines (IL-1β, IL-18, TNF-α) and enhanced anti-inflammatory IL-10, supporting a systemic shift toward an anti-inflammatory state. This dual-site effect, spanning both liver and intestine, underscores the importance of the gut–liver axis in systemic immune regulation (Xiao et al., 2024).

The basic structural foundation required to maintain appropriate barrier function is made up of intact intestinal epithelial cells. Excessive production of inflammatory cytokines compromises the intestinal mucosa by disrupting tight junction (TJ) proteins (Al-Sadi, 2009). Zn_Gly supplementation improved intestinal morphology, restored tight junction protein expression, and preserved goblet cell numbers, consistent with its role in stabilizing gut barrier integrity (Kim and Ho, 2010). By strengthening the epithelial barrier, Zn Gly likely reduced circulating endotoxins, thereby attenuating systemic inflammation and downstream hepatic damage.

LPS-induced hepatic injury is well documented and involves histopathological damage, hepatocellular apoptosis, fibrosis, and metabolic disruption (Nakadate et al., 2025). Our findings are in agreement with prior reports demonstrating that zinc acts as a cofactor for antioxidant enzymes such as SOD and metallothionein, and that glycine contributes to glutathione synthesis, together enhancing antioxidant capacity (Marreiro et al., 2017: McCarty et al., 2018). Zn_Gly supplementation reduced oxidative stress markers and improved hepatic histology, suggesting attenuation of hepatocyte apoptosis and stellate cell–driven fibrogenesis (Ghatak et al., 2011: Eron et al., 2018). These protective effects are further supported by reports that organic trace minerals, including zinc, increase hepatic antioxidant enzyme activity and improve lipid metabolism (Xu et al., 2024). This synergy was proposed to explain the more pronounced protective effects of Zn_Gly observed in this study by improving hepatic lipid metabolism through the decreased expression of FAS and ACC, along with the increased expression of CPT1a, MTTP, PPARα) and ApoB. Importantly, dietary supplementation with Zn_Gly significantly mitigated these pathological changes through inhibiting oxidative stress, systemic inflammation and apoptosis process in liver by increasing antioxidant defense mechanism.

A key factor in transcription that mediates responses of inflammation during systemic inflammation and is essential for liver injury is NF-κB. Upon activation by stimuli such as lipopolysaccharide (LPS), Pro-inflammatory genes are expressed when NF-κB transfers to the nucleus., including cytokines like tumor necrosis factor-alpha (TNF-α), interleukin-1 beta (IL-1β), and interleukin-6 (IL-6), which exacerbate hepatic inflammation and promote hepatocyte apoptosis (Zhang et al., 2020). Chronic activation of NF-κB amplifies inflammatory signaling, contributing to oxidative stress and disrupting hepatic homeostasis (Uchida et al., 2020; Hong et al., 2021). Zn Gly supplementation has been shown to reduce the generation of pro-inflammatory cytokines by blocking NF-κB activation, which in turn reduces LPS-induced liver damage. The nuclear factor erythroid 2-related factor 2 (Nrf2) pathway, a crucial modulator of cellular antioxidant responses, was also activated by Zn_Gly at the same time Nrf2 activation enhances the expression of HO-1, NQO-1, and GLCM, which reduced ROS and mitigated oxidative stress in hepatocytes (Ngo and Duennwald, 2022). Combined effects regarding suppression of inflammation regulated by NF-κB and the promotion of Nrf2-driven antioxidant defense positioned Zn_Gly as a potent nutritional intervention against hepatic damage due to systemic inflammatory insults.

Conclusion

This study demonstrates, for the first time, that Zn_Gly mitigates LPS-induced liver injury and systemic inflammation in geese by targeting the gut-liver axis. Zn_Gly improves intestinal barrier integrity, reduces endotoxin translocation, and alleviates hepatic inflammation and oxidative stress. Mechanistically, it suppresses NF-κB mediated pro-inflammatory responses while activating Nrf2-driven antioxidant defenses, thereby preserving hepatocyte function and regulating lipid metabolism. These protective effects likely stem from the enhanced bioavailability of zinc via glycine chelation. Overall, our findings highlight Zn_Gly as a promising nutritional strategy for managing endotoxin-induced intestinal and hepatic dysfunction, advancing the understanding of trace mineral-based immunometabolic regulation.

CRediT authorship contribution statement

Zeshan Zulfiqar: Writing – original draft. **Muhammad Arslan Asif:** Validation. **Layla Al-Mitib:** Conceptualization. **Khawla Alharbi:** Investigation, Conceptualization. **Tanzina Hossain:** Formal analysis. **Han Yao:** Methodology. **Xiaoyan Zhu:** Validation. **Zhichang Wang:** Formal analysis. **Hao Sun:** Formal analysis. **Yalei Cui:** Formal analysis. **Boshuai Liu:** Project administration. **Yinghua Shi:** Conceptualization, Funding acquisition, Project administration, Writing – review & editing.

Disclosures

The authors declare that they have no known competing financial interests or personal relationships that could have appeared to influence the work reported in this paper.

Funding Declaration

This study was financially supported by the China Agriculture Research System of MOF and MARA (No. CARS-34) and the Science and Technology Innovation Leading Talent in Central Plains (No. 244200510010).

Consent for publication

All authors have reviewed and consented to the publication of this manuscript.

Supplementary materials

Supplementary material associated with this article can be found, in the online version, at doi:10.1016/j.psj.2025.105772.

References

Abuajamieh, M., Abdelqader, A., Irshaid, R., Hayajneh, F.M.F., Al-Khaza'leh, J.M., Al-Fataftah, A.-R., 2020. Effects of organic zinc on the performance and gut integrity of broilers under heat stress conditions. Arch. Anim. Breed. 63, 125–135.

Aksoy-Ozer, Z.B., Bitirim, C.V., Turan, B., Akcali, K.C., 2024. The role of zinc on liver fibrosis by modulating ZIP14 expression throughout epigenetic regulatory mechanisms. Biol. Trace Elem. Res. 202, 5094–5105.
Albillos, A., De Gottardi, A., Rescigno, M., 2020. The gut-liver axis in liver disease: pathophysiological basis for therapy. J. Hepatol. 72, 558–577.
Allameh, A., Niayesh-Mehr, R., Aliarab, A., Sebastiani, G., Pantopoulos, K., 2023. Oxidative stress in liver pathophysiology and disease. Antioxidants 12, 1653.
Al-Sadi, R., 2009. Mechanism of cytokine modulation of epithelial tight junction barrier. Front. Biosci. 2765.
Chand, N., Ali, P., Alhidary, I.A., Abdelrahman, M.A., Albadani, H., Khan, M.A., Seidavi, A., Laudadio, V., Tufarelli, V., Khan, R.U., 2021. Protective effect of grape (Vitis vinifera) seed powder and zinc-glycine complex on growth traits and gut health of broilers following Eimeria tenella challenge. Antibiotics 10, 186.
Chang, Y., Wang, K., Wen, M., Wu, B., Liu, G., Zhao, H., Chen, X., Cai, J., Jia, G., 2023. Organic zinc glycine chelate is better than inorganic zinc in improving growth performance of cherry valley ducks by regulating intestinal morphology, barrier function, and the gut microbiome. J. Anim. Sci. 101, skad279.
Chen, J., Li, F., Yang, W., Jiang, S., Li, Y., 2021. Comparison of gut microbiota and metabolic status of sows with different litter sizes during pregnancy. Front. Vet. Sci. 8, 793174.
Eron, S.J., MacPherson, D.J., Dagbay, K.B., Hardy, J.A., 2018. Multiple mechanisms of zinc-mediated inhibition for the apoptotic caspases-3, -6, -7, and -8. ACS Chem. Biol. 13, 1279–1290.
Ghatak, S., Biswas, A., Dhali, G.K., Chowdhury, A., Boyer, J.L., Santra, A., 2011. Oxidative stress and hepatic stellate cell activation are key events in arsenic induced liver fibrosis in mice. Toxicol. Appl. Pharmacol. 251, 59–69.
Hong, T., Chen, Y., Li, X., Lu, Y., 2021. The role and mechanism of oxidative stress and nuclear receptors in the development of NAFLD (J Pu, Ed.). Oxidat. Med. Cell. Long. 2021, 6889533.
Jarosz, Ł., Marek, A., Grądzki, Z., Kwiecień, M., Kalinowski, M., 2017. The effect of feed supplementation with zinc chelate and zinc sulphate on selected humoral and cell-mediated immune parameters and cytokine concentration in broiler chickens. Res. Vet. Sci. 112, 59–65.
Jarosz, Ł., Marek, A., Grądzki, Z., Laskowska, E., Kwiecień, M., 2019. Effect of zinc sulfate and zinc glycine chelate on concentrations of acute phase proteins in chicken serum and liver tissue. Biol. Trace Elem. Res. 187, 258–272.
Kim, Y.S., Ho, S.B., 2010. Intestinal goblet cells and mucins in health and disease: recent insights and progress. Curr. Gastroenterol. Rep. 12, 319–330.
Kusanaga, M., Oe, S., Ogino, N., Minami, S., Miyagawa, K., Honma, Y., Harada, M., 2019. Zinc attenuates the cytotoxicity of some stimuli by reducing endoplasmic reticulum stress in hepatocytes. Int. J. Mol. Sci. 20, 2192.
Ma, W., Niu, H., Feng, J., Wang, Y., Feng, J., 2011. Effects of zinc glycine chelate on oxidative stress, contents of trace elements, and intestinal morphology in broilers. Biol. Trace Elem. Res. 142, 546–556.
Marreiro, D., Cruz, K., Morais, J., Beserra, J., Severo, J., De Oliveira, A., 2017. Zinc and oxidative stress: current mechanisms. Antioxidants 6, 24.
Martins, M.D.P.S.C., Oliveira, A.S.D.S.S., Martins, M.D.C.D.C.E., Carvalho, V.B.L.D., Rodrigues, L.A.R.L., Arcanjo, D.D.R., Santos, M.A.P.D., Machado, J.S.R., De Moura Rocha, M., 2022. Effects of zinc supplementation on glycemic control and oxidative stress in experimental diabetes: a systematic review. Clin. Nutr. ESPEN 51, 28–36.
McCarty, M.F., O'Keefe, J.H., DiNicolantonio, J.J., 2018. Dietary glycine is rate-limiting for glutathione synthesis and may have broad potential for health protection. Ochsner J. 18, 81–87.
Mohammad, M.K., Zhou, Z., Cave, M., Barve, A., McClain, C.J., 2012. Zinc and liver disease. Nut Clin. Prac. 27, 8–20.
Nakadate, K., Saitoh, H., Sakaguchi, M., Miruno, F., Muramatsu, N., Ito, N., Tadokoro, K., Kawakami, K., 2025. Advances in understanding lipopolysaccharide-mediated Hepatitis: mechanisms and pathological features. CIMB 47, 79.
Ngo, V., Duennwald, M.L., 2022. Nrf2 and oxidative stress: a general overview of mechanisms and implications in Human disease. Antioxidants 11, 2345.
Prasad, A.S., Bao, B., 2019. Molecular mechanisms of zinc as a pro-antioxidant mediator: clinical therapeutic implications. Antioxidants 8, 164.
Ren, Y., Sun, Y., Javad, H.U., Wang, R., Zhou, Z., Huang, Y., Shu, X., Li, C., 2024. Growth performance of and liver function in heat-stressed Magang Geese fed the antioxidant zinc ascorbate and its potential mechanism of action. Biol. Trace Elem. Res. 203, 1035–1047.
Tonelli, C., Chio, I.I.C., Tuveson, D.A., 2018. Transcriptional regulation by Nrf2. Antioxid. Redox Signal. 29, 1727–1745.
Uchida, D., Takaki, A., Oyama, A., Adachi, T., Wada, N., Onishi, H., Okada, H., 2020. Oxidative stress management in chronic liver diseases and hepatocellular carcinoma. Nutrients 12, 1576.
Vicuña, E.A., Kuttappan, V.A., Galarza-Seeber, R., Latorre, J.D., Faulkner, O.B., Hargis, B.M., Tellez, G., Bielke, L.R., 2015. Effect of dexamethasone in feed on intestinal permeability, differential white blood cell counts, and immune organs in broiler chicks. Poult. Sci. 94, 2075–2080.
Von Bülow, V., Dubben, S., Engelhardt, G., Hebel, S., Plümäkers, B., Heine, H., Rink, L., Haase, H., 2007. Zinc-dependent suppression of TNF-α production is mediated by protein kinase A-induced inhibition of raf-1, iκb kinase β, and NF-κb. J. Immunol. 179, 4180–4186.
Wang, S., Zhang, K., Song, X., Huang, Q., Lin, S., Deng, S., Qi, M., Yang, Y., Lu, Q., Zhao, D., Meng, F., Li, J., Lian, Z., Luo, C., Yao, Y., 2023. TLR4 Overexpression aggravates bacterial lipopolysaccharide-induced apoptosis via excessive autophagy and NF-κb/MAPK signaling in transgenic mammal models. Cells 12, 1769.
Wessels, I., Maywald, M., Rink, L., 2017. Zinc as a gatekeeper of immune function. Nutrients 9, 1286.
Xiao, C., Comer, L., Pan, X., Everaert, N., Schroyen, M., Song, Z., 2024. Zinc glycinate alleviates LPS-induced inflammation and intestinal barrier disruption in chicken embryos by regulating zinc homeostasis and TLR4/NF-κb pathway. Ecotoxicol. Environ. Saf. 272, 116111.
Xie, Y., Wen, M., Zhao, H., Liu, G., Chen, X., Tian, G., Cai, J., Jia, G., 2021. Effect of zinc supplementation on growth performance, intestinal development, and intestinal barrier function in Pekin ducks with lipopolysaccharide challenge. Poult. Sci. 100, 101462.
Xu, W., Zhou, M., Yang, Z., Zheng, M., Chen, Q., 2024. Organic trace elements enhance growth performance, antioxidant capacity, and gut microbiota in finishing pigs. Front. Vet. Sci. 11, 1517976.
Zhang, T., Ma, C., Zhang, Z., Zhang, H., Hu, H., 2021. NF-κb signaling in inflammation and cancer. MedComm 2, 618–653.
Zhang, L., Wang, J.-S., Wang, Q., Li, K.-X., Guo, T.-Y., Xiao, X., Wang, Y.-X., Zhan, X.-A., 2018. Effects of maternal zinc glycine on mortality, zinc concentration, and antioxidant status in a developing embryo and 1-day-old chick. Biol. Trace Elem. Res. 181, 323–330.
Zhang, J., Wieser, A., Lin, H., Fan, Y., Li, H., Schiergens, T.S., Mayerle, J., Gerbes, A.L., Steib, C.J., 2020. Pretreatment with zinc protects Kupffer cells following administration of microbial products. Biomed. Pharmacother. 127, 110208.
Zhong, Z., Wheeler, M.D., Li, X., Froh, M., Schemmer, P., Yin, M., Bunzendaul, H., Bradford, B., Lemasters, J.J., 2003. L-glycine: a novel antiinflammatory, immunomodulatory, and cytoprotective agent. Curr. Opin. Clin. Nutr. Metab. Care 6, 229–240.
Zulfiqar, Z., Asif, M.A., Liu, M., Zhang, S., Naeini, H.R.R., Cui, Y., Liu, B., Shi, Y., 2025. Zinc glycine supplementation improves bone quality in meat geese by modulating gut microbiota, SCFA's, and gut barrier function through Wnt10b/NF-κb axis. Poult. Sci. 104, 104925.